

# **Effects of Pore Fluid and Surface Roughness on Geomembrane - Soil Interface Behavior**

**Inci DEVELIOGLU<sup>1</sup>**  
**Hasan Firat PULAT<sup>2</sup>**

## **ABSTRACT**

In this study, direct shear tests were conducted on soil - geomembrane interfaces. Sand/bentonite mixture and crushed sand were tested in contact with two geomembranes of the same type. To examine the effect of leachate on the mechanical properties of the geomembrane, acidic mine drainage, coal combustion product, and municipal solid waste leachates were prepared in the laboratory. The initial void ratio and internal friction angles of sand/bentonite and crushed sand were 0.34, 0.52, and 23°, 35°, respectively. In the smooth geomembrane - soil interface, the minimum interface friction angle (18°) was obtained on acidic mine drainage cured geomembrane - sand/bentonite, while the maximum (31°) interface friction angle was obtained on uncured geomembrane - crushed sand. In the textured geomembrane - soil interface, the minimum interface friction angle (17°) was obtained on acidic mine drainage cured geomembrane - sand/bentonite, while the maximum (43°) interface friction angle was obtained on uncured geomembrane - crushed sand. The friction angle of the crushed sand - geomembrane surface is higher than the friction angle of the sand/bentonite - geomembrane surface. While acidic mine drainage is the leachate that affects the shearing behavior of the geomembrane in the most negative way, coal combustion product is the leachate that has the least negative impact.

**Keywords:** Geomembrane, interface shear strength, leachate, direct shear test.

## **1. INTRODUCTION**

Geosynthetics (GSs) are planar products made from polymers that have a widespread application in environmental and geotechnical engineering. Most parts of a modern landfill design are used as linings to prevent leachate from accumulating and leaking polluting the environment [1 – 3]. Storage of different solid waste (municipal, mine, coal, etc.) has become a common application in recent years [4 – 5]. However, disposal areas should be designed in

---

Note:

- This paper was received on May 19, 2022 and accepted for publication by the Editorial Board on December 16, 2022.
  - Discussions on this paper will be accepted by May 31, 2023.
- <https://doi.org/10.18400/tjce.1224424>

1 Izmir Katip Celebi University, Department of Civil Engineering, Izmir, Türkiye  
inci.develioglu@ikcu.edu.tr - <https://orcid.org/0000-0001-6594-8095>

2 Izmir Katip Celebi University, Department of Civil Engineering, Izmir, Türkiye  
hfirat.pulat@ikcu.edu.tr - <https://orcid.org/0000-0002-8298-7106>

such a way that they do not pose a problem for the environment and human health [6 – 8]. Specially produced cover composite and lining systems should be placed on the base of the landfill and over the waste. These systems usually consist of multiple hydraulic barriers made up of layers of geomembrane (GM) or geosynthetic clay liner (GCL). Two kinds of GCL are generally used in geosynthetic composite systems in landfills; the unreinforced GCL containing a thin layer of bentonite bonded to high-density polyethylene (HDPE) GM, and the reinforced GCL containing a stitched or needle punched geotextile encapsulated bentonite to bond the support geotextiles [9 – 10]. Generally, textured HDPE geomembrane is preferred in systems used with geotextiles. On these barriers, sand or gravel is laid as the last layer [11 – 12].

Lateral shear stresses that can occur under the influence of lateral forces such as earthquake winds, etc., were not taken into account in the designs, which led to various construction errors, such as the shearing of the storage facility in Kettleman Hills, California [13]. Landfill covers (protection covers) used today effectively fulfill their duties. However, how long these systems can maintain their efficiency should be examined in detail. For this reason, it is necessary to elaborate examine its mechanical properties in detail. Although there are many studies on permeability, puncture, and tearing in the literature, studies examining mechanical properties under the influence of lateral stresses are quite limited [14 – 16]. As a result of the studies, it was determined that this disaster occurred due to the shear failure at the soil – GM interface. Due to limited references, engineers usually reduce the internal friction angle by a little ( $1/2$  or  $2/3$ ) when obtaining the interface friction angle as recommended in textbooks [17]. Some researchers have determined that these coefficients may be less than  $2/3$  or even less than  $1/2$  in their studies, so the interface behavior between different soils and different geomembranes needs to be examined in detail [18 – 19].

In the literature, some studies examined the effect of only soil type or only geomembrane type on the interface shear behavior. Chai and Saito [20] determined the geomembrane – clay interface shear strength behavior with a large-scale direct shear device. Bentonite powder and quartz (30%) were mixed with clayey soil (70%). The types of geomembranes used in the study are polyvinyl chloride (PVC), polyethylene (PE), and high-density polyethylene (HDPE). Direct shear tests were conducted under the 50, 80, and 100 kPa normal stresses. The test results showed that the clayey soil – PVC interface had a maximum adhesion value. The interface friction angle between bentonite and all other geomembranes was quite small ( $3^\circ$  -  $4^\circ$ ). Since the water coming out of the bentonite accumulates at the interface during the shear test, a water layer is formed between the geomembrane and the bentonite particles, and therefore the interface friction angle is lower than it should be. Besides, the shear strength of the soil was achieved approximately 55% bigger than the interface shear strength. Effendi [18] studied the interface shear strength behaviors of different types of geomembranes (smooth HDPE, very smooth LDPE, PVC) and Ottawa sand. The geomembrane thicknesses were 2.03, 1.52, and 1.52 mm, respectively. The interface shear strength parameters were determined by the ring shear test, the normal stresses ranged from 50 kPa to 200 kPa, and the shear rate was 2.4 mm/min. The productivity ratio [E] ( $\tan\delta/\tan\phi$ ) was derived to evaluate the results obtained. The HDPE with a very stiff and smooth surface had the lowest from 34 to 45% ( $E = 0.34$  to  $0.45$ ). A higher between 44 to 59% of that of the Ottawa sand was mobilized in the tests with the relatively softer surface VLDPE geomembrane. For PVC geomembrane the productivity ratio ranged between 70 to 97% of the Ottawa sand at normal stress from 50 kPa to 223 kPa. In conclusion, the interface strength of these smooth

geomembranes was found to be dependent on normal stress levels: the PVC was the most dependent, and the smooth HDPE was the least dependent. Feng and Cheng [9] conducted laboratory tests to obtain the interface shear strength behaviors between geomembrane – soil and geomembrane – geotextile. These experiments were repeated more than once under different normal stresses. A 1.5 mm thick textured HDPE geomembrane and nonwoven geotextile with a mass per unit area of 400 g/m<sup>2</sup> were used. The soil was classified as silty clay with silty sand according to USCS. The shear strength experiments were conducted with a large-scale direct shear and the shear rate was 1 mm/min. For the geomembrane – geotextile interface, one sample was tested under increasing normal stress with the order of 50, 100, and 200 kPa. For geomembrane – soil interface experiments, five specimens were examined three times under constant normal stress of 20, 50, 100, 200, and 300 kPa. One sample was sheared three times at increasing normal stress from 50 to 100 and 200 kPa. The geomembrane – geotextile interface friction angle values were found 19.8°, 18.07°, and 17.45° for the 1<sup>st</sup>, 2<sup>nd</sup>, and 3<sup>rd</sup> repeat, respectively. The geomembrane – soil interface friction angle values were found 10.67°, 9.07°, and 9.00° for the 1<sup>st</sup>, 2<sup>nd</sup>, and 3<sup>rd</sup> repeat, respectively. Geomembranes are exposed to various leachates in storage facilities. These leachates damage the geomembranes over time due to the chemicals they contain. In the literature, there are studies examining the damage of leachates on geomembranes. Stark and Santoyo [21] investigated the interface shear strength behavior between ten geomembranes and two soils. Seven geomembranes are smooth, three are textured and their thickness varies between 0.75 and 1.5 mm. The types of geomembrane used are PVC, HDPE, LLDPE, coated woven polyethylene and polyolefin. The types of soil used were clayey glacial till and Ottawa fine sand. The interface shear strength parameters were measured with a torsional ring shear apparatus and the shear rate was 0.015 mm/min. The results of the experimental study showed that textured geomembranes have a larger interface friction angle than smooth geomembranes. According to clayey glacial till soil tests, the maximum interface friction angle (46°) was obtained tenth GM (textured, 1.5 mm, HDPE). The minimum interface friction angle (14°) was obtained ninth GM (smooth, 1.5 mm, HDPE). According to Ottawa sand soil tests, the maximum interface friction angle (31°) was obtained tenth GM (textured, 1.5 mm, HDPE). The minimum interface friction angle (15°) was obtained second GM (smooth, 1.5 mm, LLDPE). Also, the glacial till/geomembrane interfaces exhibited higher interface friction angles than the Ottawa Sand/geomembrane interfaces. Abdelaal et al. [22] investigated the effect of leachate constituents on the oxidation induction time (OIT) and physical properties of geomembrane. The leachate was obtained by mixing various chemicals in the laboratory to represent municipal solid waste leachate. The geomembranes were kept in glass pools containing these leachates for about 108 months at different temperatures (22, 40, 55, 70, and 85 °C). Melt index, stress-crack resistance, and OIT tests were performed on the samples that completed the curing period. At the end of 4 months, the OIT value decreased by 98% at 85 °C and by 40% at 55 °C. There was a decrease in melting index at 55 °C to reach almost 0.8 (from 1.0) after 25 months and then the values increase with time to the initial values after 75 months of incubation. Similar trends were obtained at other temperatures. On the other hand, a sharp decrease was observed in the stress-crack resistance at the end of 80 months at 55 °C, 40 months at 70 °C, and 12 months at 85 °C. Gulec et al. [23] examined the effect of acidic mine drainage (AMD) leachate on the mechanical properties of the HDPE geomembrane. The geosynthetic materials were immersed in tanks containing synthetic AMD at 20, 40, or 60 °C over 22 months. According to mechanical test results, that is no temporal changes in wide-strip tensile, puncture, and tear strength are

evident, regardless of the temperature or leachate. Similar results have been reported by Mitchell [24] and Grubb et al. [25] for other geomembranes exposed to AMD.

In this study, the friction angle between the soil and the geomembrane was determined using a medium-scaled direct shear device. Smooth and textured HDPE GM with a thickness of 1.5 mm was used as the GM type. Crushed sand and sand/bentonite mixture (80/20) were used because they are generally used in landfills. In addition, GMs were cured in three different synthetic leachate fluids in a laboratory environment for four months to represent the environment formed in solid waste landfills more meaningfully. These fluids were leachates of municipal solid waste (MSW), coal combustion product (CCP), and acidic mine drainage (AMD). First of all, the geotechnical index parameters and internal friction angles ( $\phi$ ) of the soils were determined. Then, the friction angles ( $\delta$ ) of the interfaces formed between the uncured and cured geomembranes and the soils were determined. This study investigated soils and geomembranes with different properties in combination under the influence of various leachates. Shear strength mechanisms were determined and material behavior was evaluated. In addition, laboratory studies were supported by microscopic image analysis. In terms of content, it is thought that study will contribute to the development of both practice and academic studies.

## 2. MATERIALS

### 2.1. Soils

Two different soils were used in this study, namely, sand/bentonite (80/20) mixture (SB: particle size 2.0 mm – 0.0 mm) and crushed sand (CS: particle size 2.0 mm – 0.075 mm). The reason why these soils were preferred was that they were frequently used in waste storage areas [26 – 27]. In addition, the effect of grain size was investigated by using such soils. The geotechnical index properties of soils have been listed in Table 1. Image analysis was

*Table 1 - Some geotechnical index properties of soils used in this study*

Property	Sand/bentonite (SB)	Crushed sand (CS)
Specific gravity, $G_s$	2.46	2.68
Liquid limit, LL (%)	60.7	-
Plastic limit, PL (%)	30.2	NP
Max. dry unit weight, $\gamma_{dry,max}$ (kN/m <sup>3</sup> )	17.0	17.3
Opt. moisture content, $w_{opt}$ (%)	13.2	11.2
D <sub>10</sub>	-	0.19
D <sub>30</sub>	0.2	0.69
D <sub>60</sub>	1.5	1.70
Coefficient of uniformity, $C_u$	-	8.95
Coefficient of curvature, $C_c$	-	1.47
USCS	SC	SW

performed with soil particles using the ImageJ software (Figure 1). As a result of the particle analysis, the roundness of the CS soil was obtained as 0.57, while the roundness of the SB soil was obtained as 0.71 (between 0-1).

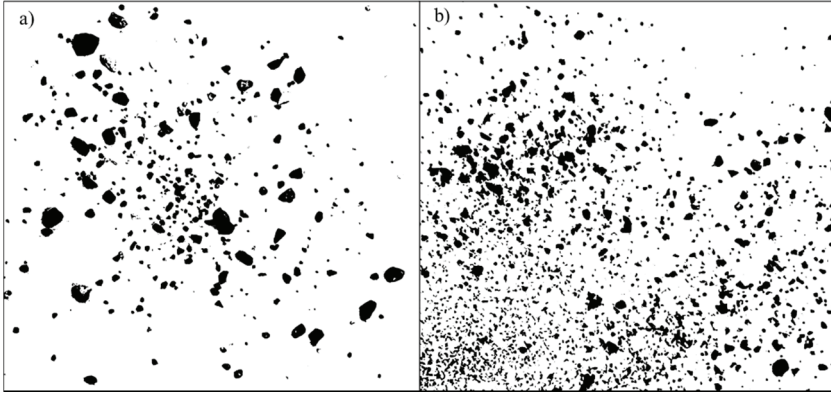


Figure 1 - Image analysis of a) CS, b) SB

## 2.2. Geomembranes

In this study, smooth (HDPE) and textured (HDPE/T) high-density polyethylenes, which are commercially available, were used. These types of GMs have a high tensile strength at low stresses, low-cost assembly, and long-term weather resistance so they are frequently preferred in applications. Polyethylene (PE) is the name of ethylene in monomer form. Ethylene turns into Polyethylene with several polymerization methods. HDPE geomembrane is a geosynthetic liner formed as a result of the extrusion of high-density polyethylene and shaped homogeneously. HDPE GMs are used for sealing in projects such as mine waste landfills, tank fields, municipal solid waste landfills, acid tanks, ponds, and irrigation canals. The properties and physical appearance of these GMs given by the manufacturer have been listed in Table 2.

Table 2 - Some characteristics of geomembranes used in this study

Essential characteristics	Unit	HDPE	HDPE/T
Thickness	mm	1.5	1.5
Stress crack resistance	h	>200	>200
Elongation at yield	%	>12	>12
Tensile stress at break	N/mm <sup>2</sup>	>26	>26
Elongation at break	%	>700	>700
Water permeability	m <sup>3</sup> /m <sup>2</sup> .d	<10 <sup>-6</sup>	<10 <sup>-6</sup>
Resistance to weathering	%	<25	<25
Oxidation strength	%	<25	<25
Yield strength	N/mm <sup>2</sup>	>16	>16
Static puncture resistance	N	3700	7200

**2.3. Synthetic Leachates**

The synthetic leachates used in this study were produced by mixing various chemical compounds in distilled water, as suggested by Hrapovic [28], Gulec et al. [23], Rowe et al. [29], and Benson et al. [30]. Three different leachates were created synthetically in the laboratory to represent solid waste landfills. These were leachates of municipal solid waste (MSW), coal combustion product (CCP), and acidic mine drainage (AMD). The MSW leachate was a suitable medium for the growth and maintenance of acetogenic, methanogenic, and sulfidogenic bacteria involved in the mineralization stage of anaerobic degradation. Also, the mixture containing only three volatile fatty acids, adjusted to pH = 3.45, was used as a possible variation of landfill leachate [31-34]. The chemical contents of the MSW leachate have been listed in Table 3.

*Table 3 - Composition of MSW leachate (Hrapovic [28])*

Chemical name	Chemical formula	Amount (per 1 L)
Acetic acid	CH <sub>3</sub> COOH	7 mL
Propionic acid	CH <sub>3</sub> CH <sub>2</sub> CO <sub>2</sub> H	5 mL
Butyric acid	C <sub>4</sub> H <sub>8</sub> O <sub>2</sub>	1 mL
Dipotassium phosphate	K <sub>2</sub> HPO <sub>4</sub>	30 mg
Potassium bicarbonate	KHCO <sub>3</sub>	312 mg
Potassium carbonate	K <sub>2</sub> CO <sub>3</sub>	324 mg
Sodium chloride	NaCl	1440 mg
Sodium nitrate	NaNO <sub>3</sub>	50 mg
Bicarbonate of Soda	NaHCO <sub>3</sub>	3012 mg
Calcium chloride	CaCl <sub>2</sub>	2882 mg
Magnesium chloride hexahydrate	MgCl <sub>2</sub> .6H <sub>2</sub> O	3114 mg
Magnesium sulfate	MgSO <sub>4</sub>	156 mg
Ammonium bicarbonate	NH <sub>4</sub> HCO <sub>3</sub>	2439 mg
Urea	CO(NH <sub>2</sub> ) <sub>2</sub>	695 mg
Trace metal solution	-	1 mL
Sodium sulfide nonahydrate	Na <sub>2</sub> S.9H <sub>2</sub> O	Titrate to an E <sub>h</sub> -120-180 mV
Sodium hydroxide	NaOH	Titrate to a pH 5.8-6.0
Distilled water	H <sub>2</sub> O	To make 1 L

The CCP leachates used in this study were identified through analysis of a database containing leachate data from 33 CCP disposal sites compiled by the Electric Power Research Institute (EPRI) [30]. The database included concentrations of major cations and anions, ionic strength, the relative abundance of monovalent and polyvalent cations, pH, and electrical conductivity (EC). It was determined that CCP leachate was slightly alkaline (pH 7.65) as a result of pH measurements. The chemical contents of the CCP leachate have been listed in Table 4.

Table 4 - Composition of CCP leachate (Benson et al. [30])

Chemical name	Chemical formula	Amount (mg)
Potassium sulfate	$K_2SO_4$	161
Sodium chloride	$NaCl$	51
Calcium chloride	$CaCl_2$	58
Sodium sulfate	$Na_2SO_4$	722
Calcium sulfate	$CaSO_4$	987
Magnesium sulfate	$MgSO_4$	146

The composition of AMD was selected by reviewing the composition of 12 AMD for metallic mine waste reported in the literature [33]. In this mixture, the most common metals (Fe, Zn, Cu, and Ca) in AMD, their concentrations and types were determined, relative. Fe, Zn, and Cu are also three of the five most abundant metals extracted from sulfide ores (Fe, Ni, Cu, Pb, and Zn). It was determined that AMD leachate was quite acidic (pH 0.95) as a result of pH measurements. The concentrations of these metals obtained from the literature have been shown in Table 5.

Table 5 - Composition of AMD leachate (Gulec et al. [33])

Chemical name	Chemical formula	Amount (mg)
Copper (II) sulfate	$CuSO_4$	88
Zinc Sulphate Heptahydrate	$ZnSO_4 \cdot 7H_2O$	864
Sulfuric Acid	$H_2SO_4$	886
Iron (II) sulfate heptahydrate	$FeSO_4 \cdot H_2O$	4076
Calcium sulfate	$CaSO_4$	681

They were replaced by fresh leachate every 2–4 weeks [33]. Direct shear tests were carried out with geomembranes that completed their curing period. When the studies in the literature were examined, it has been shown that there was a change in the mechanical properties of GMs even after 4 months of curing [35].

### 3. METHODS

#### 3.1. Direct Shear Tests

In the first phase of the laboratory experiments, the internal friction angles of the soils were determined using a medium-scale direct shear box with dimensions of 100 x 100 mm using the conventional direct shear test method according to ASTM D30808 [36], [37 – 40]. The interface friction angle ( $\delta$ ) of the soil – GM interfaces were obtained according to ASTM D5321 [41] using a medium-scale direct shear apparatus, and the test setup is shown in Figure 2.

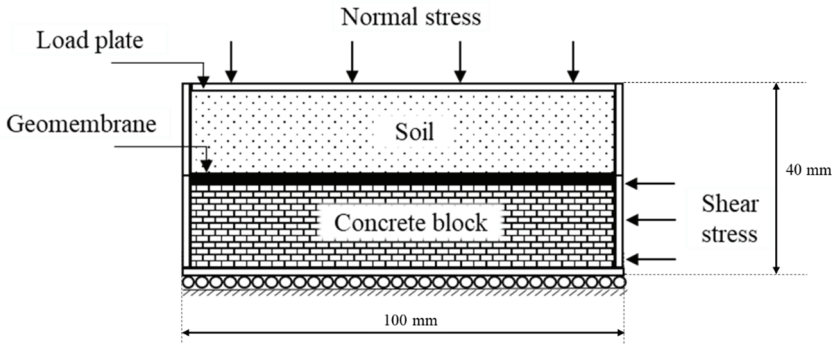


Figure 2 - Test setup of soil – GM interface direct shear test

Concrete blocks were produced in the dimensions of the lower box of the direct shear device, and this concrete block was placed in the lower box since if the soil was placed both above and below the direct shear box, the underlying soil would settle during the experiment and the geomembrane would not remain stable on the shearing surface. The geomembrane was attached to the concrete block with a strong adhesive (Mitreapel instant adhesive) to prevent the geomembrane from moving during the direct shear test. The soil was placed in the upper box of the direct shear device (Figure 3).

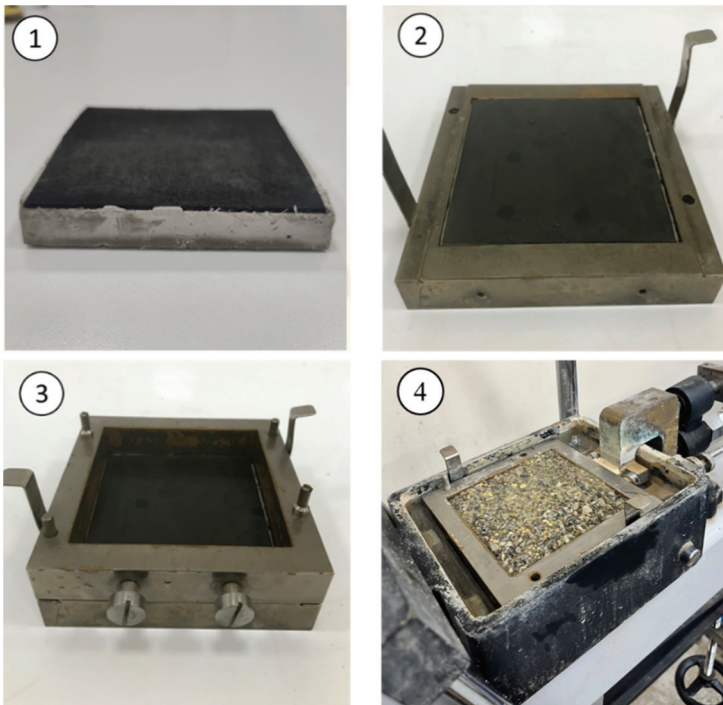


Figure 3 - Sample preparation steps for interface direct shear tests

Samples prepared at optimum water content were placed in the shear box at maximum dry unit weight density. The samples were kept in pore fluid for about two hours to achieve 100% saturation (After the experiments, the saturation degrees of the samples were almost 1). In stage I of the direct shear experiments, uncured geomembranes and tap water (TW) as pore fluid were used. In stage II, the geomembranes were kept in different leachate for 4 months, and then in the direct shear tests, these geomembranes were used. Medium-scale direct shear tests were carried out under the normal stress values of 49, 98, and 196 kPa. The experiments were carried out with a shear rate of 0.5 mm/min due to the very high permeability of CS, and 0.1 mm/min due to the low permeability of SB [20, 42].

### **3.2. Surface Roughness Measurement**

First, Koerner [43] indicated that surface roughness measurements can be used as a textural index or a textural descriptor for manufacturing quality control and construction quality assurance. However, today, high-precision measurement techniques have proven that surface roughness measurements of geomembranes are not only quality descriptors for geomembranes but may be related to various soil-geosynthetic interaction mechanisms. The Optical Profilometer method (OPM) used to measure geomembrane surface roughness is based on the theoretical developments of Gokhale and Underwood [44] and the experimental work of Gokhale and Drury [45]. The surface roughness of the samples was measured with

an optical profilometer (OPM) after direct shear tests to determine the damage caused by the leachates on the surface of the geomembranes. A profilometer is a measuring instrument used to measure a surface's profile, to quantify its roughness. Critical dimensions such as step, curvature, and flatness are computed from the surface topography. The OPM analysis was conducted in Totomak A.Ş. with a profilometer device (Figure 4). Measurements were made from an area of 4 cm<sup>2</sup> in the middle of the geomembrane, both in the shear direction and perpendicular to the shear direction. The  $R_{max}$  value was calculated by taking the average of the two measurements.

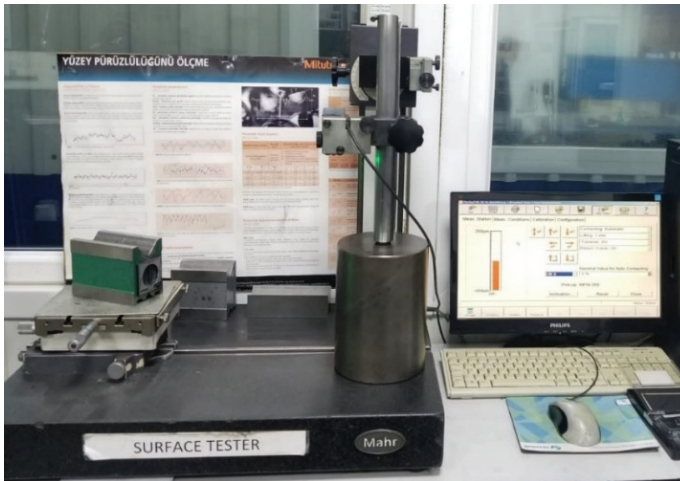


*Figure 4 - Profilometer device*

## **4. RESULTS AND DISCUSSION**

### **4.1. Direct Shear Test**

In order to determine the shear strength behavior, a conventional direct shear test (soil – soil interface) was carried out with two soils (SB, CS) prepared at the maximum dry unit weight and optimum moisture content under three normal stresses (49, 98, 196 kPa). The initial void ratio and internal friction angles of SB and CS were 0.339, 0.517, and 22.8, 34.7°, respectively. The interface friction angle values of the coarse soils were obtained higher. In the literature, as the particle size increased, the internal friction angle also increased because larger particles would require more frictional force to reach the sliding state and roll after being released at the lock peak [9, 46 – 47].

### **4.2. Interface Direct Shear Test**

Interface direct shear tests were carried out to determine the effect of the particle size, the roughness of GM, and pore fluid on the interface shear behavior between soil – GM. The preparation steps and applied normal stresses of the samples are the same as for the traditional direct shear test. The repeatability of the laboratory experimental results in direct shear and interface direct shear tests was ensured by running two to three trials from multiple tests. The shear stress-strain graphs of soil – HDPE GM and soil – HDPE/T GM have been shown in Figure 5.

In Figure 5, shear stresses at the SB-HDPE interface, all curves up to 1% strain reaches the maximum and at the same time the final value. And there was an increase in shear stress parallel to the increase in normal stress. Shear stresses at the SB-HDPE/T and CS-HDPE/T, the effect of the surface roughness of the geomembrane was seen. The curves increased up to much larger strains, notably the final value for SB was not obtained. This situation can be explained as follows, the notches of the textured GM and the soil particles are interlocked during shearing so that the shear stresses increase for a long time and then take a constant value. On the other hand, in a smooth geomembrane, the soil particles adhere to the GM surface for a while and then slide on the smooth surface, causing shear stresses to increase and then fixate [1, 18, 48]. Also, for two soil types, the soil – HDPE/T shear strength has been determined greater than the soil – HDPE shear strength. This is already an expected result because the roughness on the GM surface increases the friction force and therefore the interface friction angle also increases. The same results were obtained by Vaid and Rinne [49] and Monteiro et al. [50]. The behavior of the smooth HDPE GM was an appearance of little or no hook-and-loop interaction between the soil – smooth HDPE GM. Conversely, at the soil – textured HDPE GM interface there was a significant hook-and-loop interaction and as the roughness increased, additional passive resistances were activated [51]. Envelopes of soil – HDPE and soil – HDPE/T interfaces obtained from shear stress-strain graphs have been presented in Figure 6.

While the interface shear strengths of SB and CS were almost the same at low normal stresses, it is seen that CS had greater shear strengths than SB as the normal stress increased. The shearing resistance of the interface is caused by the sliding, and rolling of soil particles, adhesion, interlocking of soil particles with the GM surface, or embedding of soil particles into the GM. For granular soil-GM, the cohesive force corresponds to the force required to

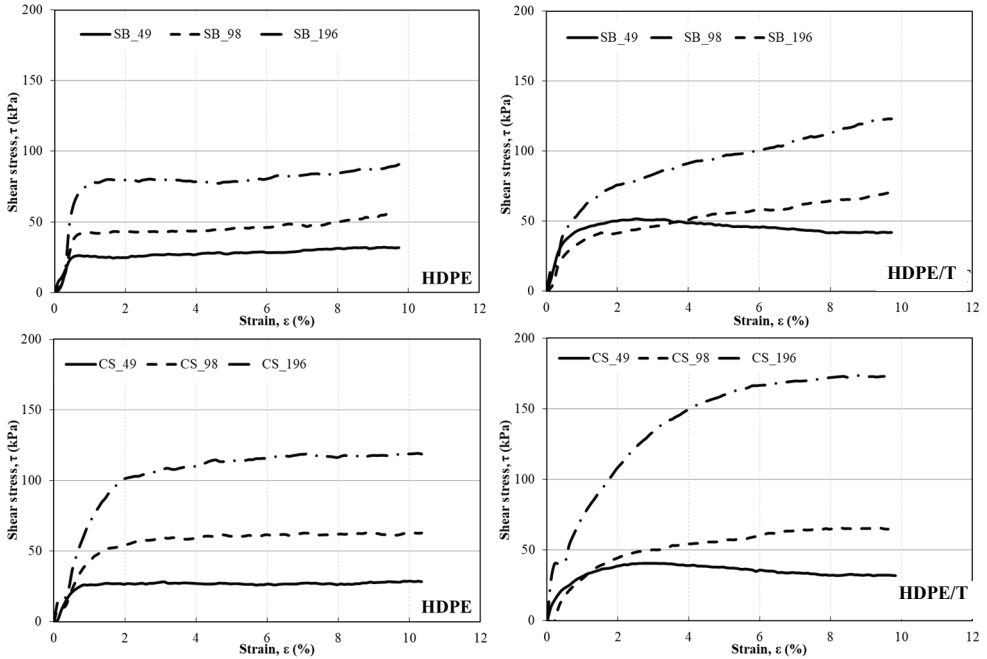


Figure 5 - Shear stress-strain graphs of soil – geomembrane interfaces

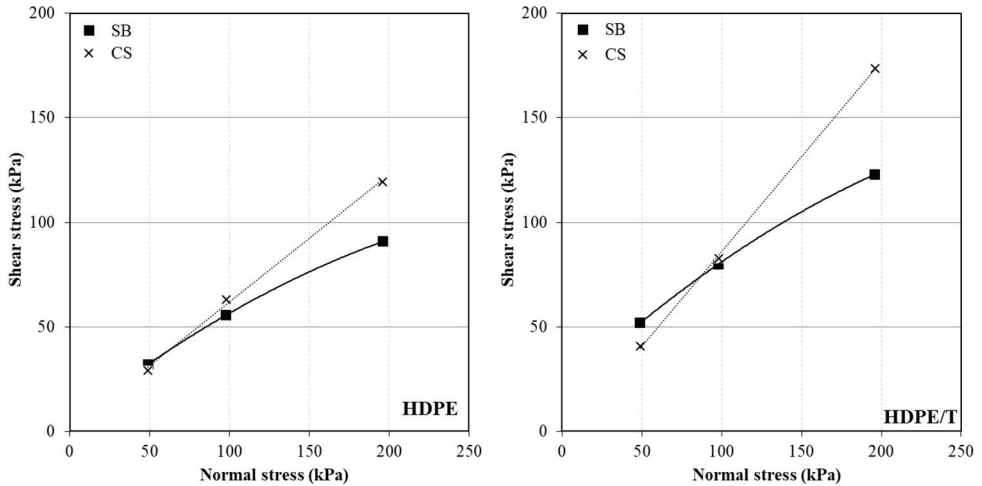


Figure 6 - Mohr-Coulomb failure envelopes of soil – geomembrane interfaces a) HDPE, b) HDPE/T

allow soil particles to slide across the interface. As the normal stress increases, so does the ability of soil particles to plow the GM. Therefore, both sliding and plowing can contribute to the overall frictional force when shearing granular soil-GM. However, the same is not true

for cohesive soils. Even under high normal stresses, they only slide, not plow [52]. This is an explanatory feature for CS with angular particles to have high shear strength. This also explains why the SB-HDPE interface has a parabolic envelope while the CS-HDPE interface has a linear envelope. In the literature, while drawing Mohr-Coulomb failure envelopes, researchers have used linear failure envelopes [53 – 54], while other researchers have to plot curved failure envelopes for cohesive soil-GM interfaces [55 – 56]. Markou and Evangelou [57] obtained the failure envelopes of the cohesive soil-GM as parabolic, while the failure envelopes of the granular soil-GM were linear.

### **4.3. Effect of Pore Fluid**

Geomembranes were stored in different leachates for 4 months in order to examine the effects of leachate generated in landfills on the shear strength parameters of the geomembranes. Interface direct shear tests were performed without curing samples in tap water (TW) and 4 months cured samples in leachates (AMD, CCP, MSW). In addition, the surface roughness of the samples was measured with a profilometer after direct shear tests to determine the damage caused by the leachates on the surface of the geomembranes.  $R_{\max}$  value, which is a surface roughness coefficient, was obtained from profilometer measurements. A comparison of the interface friction angles and  $R_{\max}$  values for different pore fluids has been shown in Figure 7.

From Figure 7, it is seen that there is no general trend between the leachate and friction angles. However, in general, AMD was the leachate that most negatively affected the friction angles, while CCP was the leachate that had the least effect. The reason why **AMD** damages the geomembrane is that chemical degradation begins with a change in polymer structure and ends with a change in engineering properties [58]. Diffuse changes in the polymer; a decrease or increase in molecular weight, embrittlement, loss of additives and plasticizers, formation of free radicals, and deterioration of transparency [59]. The reason why **MSW** damages the geomembrane is that oxidative degradation begins. Viebke et al. [60] and Hsuan and Koerner [58] described oxidative degradation as a three-step process. In stage 1, there is no significant change in the engineering properties. Stage 2 is an induction time for degradation to begin and begins after the antioxidants are depleted. In stage 3, there are significant changes in physical and mechanical properties due to oxidation. In this study, it is seen that stage 2 started after a 4-month curing period. The reason **CCP** is less harmful than others is that CCP leachates are inorganic and may have more polyvalent cations and higher ionic strength than MSW [61-62]. It also has a much higher pH than AMD. Therefore, the effect of CCP to damage the mechanical properties of the geomembrane is very low compared to AMD and MSW.

Also from Figure 7, it has been determined that the interface friction angle is inversely proportional to the scratches and grooves formed on the surface during the experiment. In order to see these scratches and grooves more clearly, microscopic images of the geomembranes were obtained after the experiment (Figure 8). While there were no scratches on the geomembrane surface before the experiment, the scratches on the surface were observed after the experiment. In addition, it was determined that the geomembrane at the HDPE-CS interface had deeper and more numerous scratches than the geomembrane at the HDPE-SB interface.

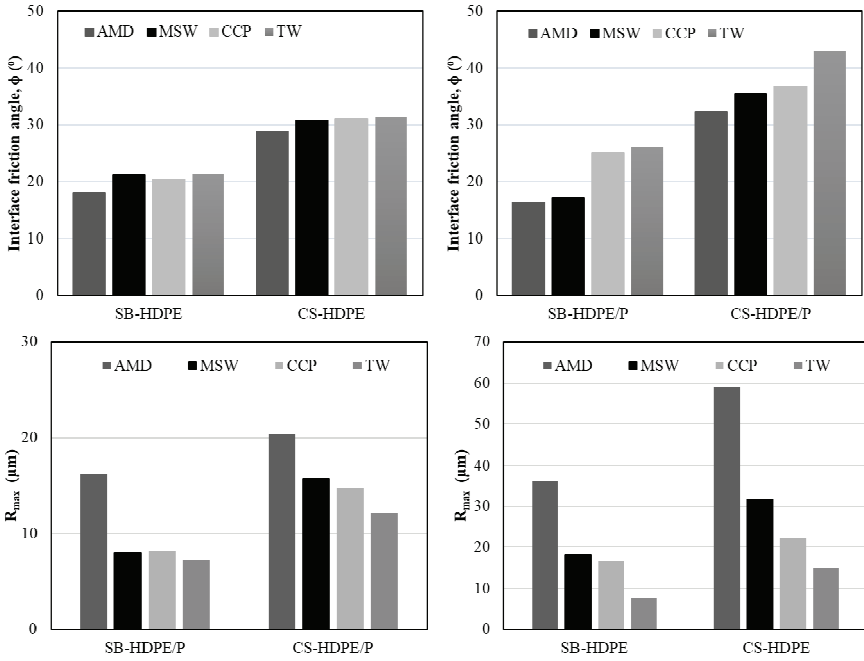


Figure 7 - Interface friction angles and  $R_{max}$  values of cured samples

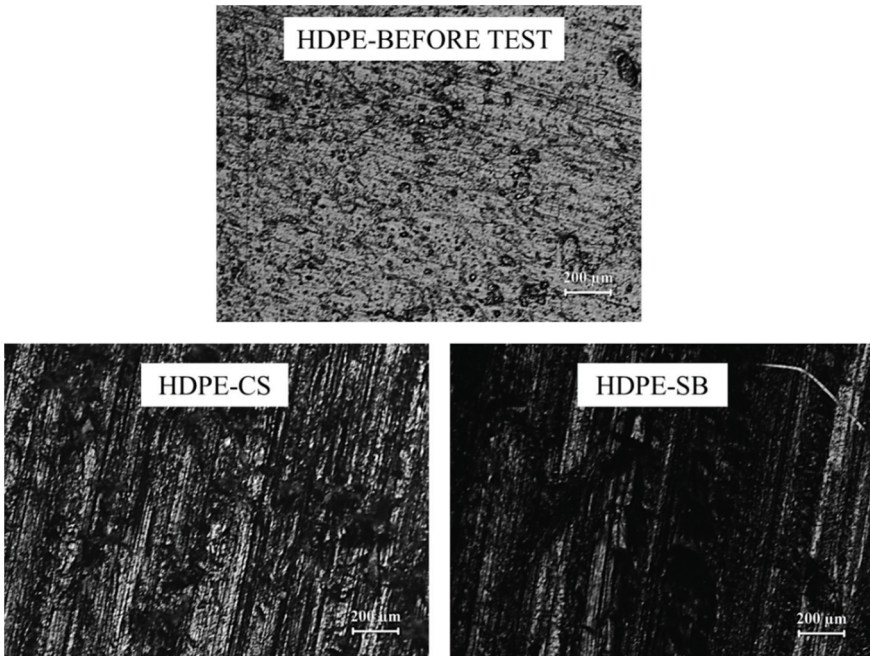


Figure 8 - Microscopic images of HDPE – soil interface

#### 4.4. Effect of Particle Size

The interface friction angle values of soil – HDPE, and soil – HDPE/T GMs have been given in Figure 9. It was found that the interface friction angles of the SB were lower than the CS. Because relatively larger particles need more frictional force to reach sliding conditions and to roll after the release of interlocking [36]. CS is less spherical, less rounded, and less regular compared to SB. These angular sand particles can form deeper grooves and plow to afford a higher interface friction angle [46, 52, 63 – 64]. It has also been reported in studies that higher interfacial friction angle values are obtained at higher dry densities by Fleming et al. [48], Adamska [65], and Khilnani et al. [66]. This is because more soil grains are in contact with the surface of the GM, resulting in increased contact area and accordingly increased interface shear strength. Also, the same conclusion was reached as a result of this study.

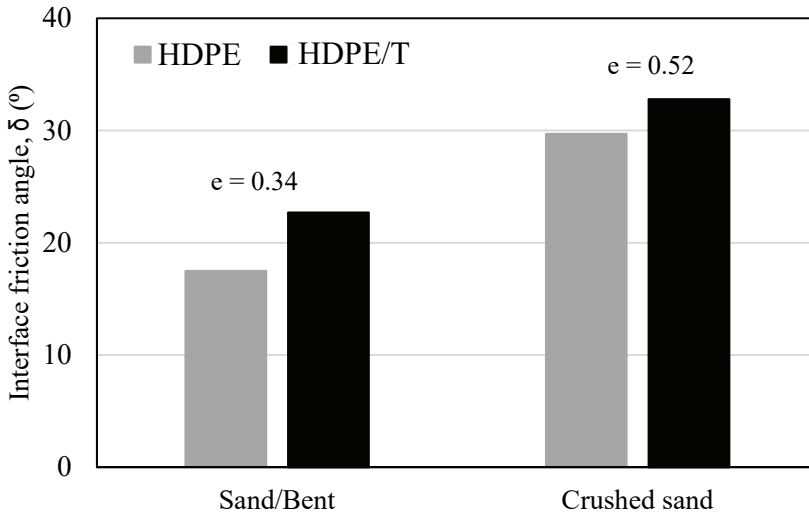


Figure 9 - The interface friction angle values of soil-HDPE and soil-HDPE/P in TW

#### 4.5. Comparison with the Literature Studies

Isaev and Sharafutdinov (2020) investigated the interface shear behavior between clayey and sandy soils and concrete, steel (polished and rough) and polymer surfaces. The  $R_{int}$  coefficient was determined by dividing the interface shear strength to the internal shear strength. The coefficients in sandy soil were 0.47-0.78, 0.47, and 0.93 for steel (polished-rough), concrete and polymer, respectively. The coefficients in clayey soil were 0.65, 0.53, and 1.0 for steel (polished), concrete and polymer, respectively [67]. In the present study, the interface-to-internal friction angle ratio of SB-HDPE and CS-HDPE was 0.94 and 0.96 in uncured experiments. The interface-to-internal friction angle ratio of SB-HDPE/T and CS-HDPE/T was 1.17 and 1.19. When compared with the results obtained from this study, it is seen that the closest result is with polymer interfaces. Considering that HDPE GM is a polymer-based material, the results obtained in this study were found to be compatible with the literature. In another study, Cen et al. (2020) investigated the dynamic shear behavior of pure sand and textured and smooth HDPE geomembrane interface. The interface peak shear

strength/internal peak shear strength ratios are 0.61 and 0.89 for smooth and rough GM, respectively [68]. When compared with the results obtained from this study, it is seen that the ratios are lower. This is because the particles of the pure sand used are more rounded and also because the GMs have lower roughness. Cabalar (2016) obtained the interface friction angles between two different sands (Trakya sand [TS] and crushed stone sand [CSS]) and steel, concrete, and wood. The ratio of the interface friction angle to the internal friction angle in TS was obtained as 0.38, 1.06, and 0.81 for steel, concrete, and wood, respectively. The ratio of the interface friction angle to the internal friction angle in CSS was obtained as 0.34, 1.14, and 0.86 for steel, concrete, and wood, respectively [69]. Compared to the results obtained from this study, the concrete interface coefficient is compatible with HDPE/T, while wood is compatible with HDPE.

## 5. CONCLUSION

In this study the interface shear strength parameters of the soil – geomembrane were investigated. The interface friction angles of the soil – geomembrane interface were obtained with a medium-scale direct shear device. Two types of soils (sand/bentonite mixture, and crushed sand) were used in the tests to investigate the effect of particle size and angularity on the interface friction angle. Smooth and textured HDPE GMs of the same thickness were used to determine the effect of the geomembrane roughness on the interface friction angle. In addition, the interface direct shear tests were also performed with 4 months cured samples in different leachates (AMD, CCP, MSW) to determine the effect of the chemical content of the leachates. As a result of the study:

- The initial void ratio and internal friction angles of SB and CS were 0.34, 0.52, and 23, 35°, respectively.
- In HDPE-soil interface, the minimum interface friction angle (18°) was obtained on AMD cured GM-SB, while the maximum (31°) interface friction angle was obtained on uncured GM-CS.
- In HDPE/P-soil interface, the minimum interface friction angle (17°) was obtained on AMD cured GM-SB, while the maximum (43°) interface friction angle was obtained on uncured GM-CS.
- It was determined that shear stress increased with increasing horizontal displacement in textured HDPE-GM interfaces, but shear stress increased up to a certain horizontal displacement and then remained constant in smooth HDPE-GM interfaces.
- Soils with larger and more angular particles have higher **interface friction angles**.
- While granular soil-geomembrane interfaces have linear Mohr-Coulomb failure envelopes, cohesive soil-geomembrane interfaces have parabolic Mohr-Coulomb failure envelopes.
- In general, it has been determined that the leachate that affects the geomembranes most **adversely** is **AMD**, and the one that affects the geomembranes the **least** is **CCP**.
- It is recommended to avoid the use of smooth and textured HDPE GMs in mine tailing storage facilities using SB and CS.
- It is recommended to use smooth HDPE GMs in coal combustion waste storages and textured HDPE GMs in municipal solid waste storages.

**Symbols**

<b>AMD</b>	Acidic mine drainage
<b>C<sub>c</sub></b>	Coefficient of curvature
<b>CCP</b>	Coal combustion product
<b>CS</b>	Crushed sand
<b>C<sub>u</sub></b>	Coefficient of uniformity
<b>E</b>	Productivity ratio
<b>EC</b>	Electrical conductivity
<b>GCL</b>	Geosynthetic clay liner
<b>GM</b>	Geomembrane
<b>GS</b>	Geosynthetic
<b>G<sub>s</sub></b>	Specific gravity
<b>HDPE</b>	Smooth high density polyethylene
<b>HDPE/T</b>	Textured high density polyethylene
<b>LDPE</b>	Low density polyethylene
<b>LL</b>	Liquid limit
<b>MSW</b>	Municipal solid waste
<b>OIT</b>	Oxidation induction time
<b>OPM</b>	Optical profilometer
<b>PE</b>	Polyethylene
<b>PL</b>	Plastic limit
<b>PVC</b>	Polyvinyl chloride
<b>SB</b>	Sand/Bentonite mixture
<b>TW</b>	Tap water
<b>USCS</b>	Unified soil classification system
<b>VLDPE</b>	Very low density polyethylene
<b>w<sub>opt</sub></b>	Optimum water content
<b>γ<sub>dry,max</sub></b>	Maximum dry density
<b>δ</b>	Interface friction angle
<b>φ</b>	Internal friction angle

## **Acknowledgments**

We gratefully thank the companies of Geoplas Plastik Zemin Teknikleri Ve Kimya San.Tic.Ltd.Şti. and Totomak Makina ve Yedek Parça Sanayi ve Ticaret A.Ş.

## **Funding**

This work was supported by the TUBITAK 2211-A education scholarship program.

## **References**

- [1] Bonnour, H., Barral, C., Touze-Foltz, N. Altered geosynthetic clay liners: effect on the hydraulic performance of composite liners. *Europ. J. Environ. Civ. Eng.*, 19(9), 1155 – 1176, 2015. <https://doi.org/10.1080/19648189.2015.1005161>.
- [2] Sabiri ,N.E., Caylet, A., Montillet, A., Le Coq, L., Durkheim, Y. Performance of nonwoven geotextiles on soil drainage and filtration. *Europ. J. Environ. Civ. Eng.*, 24(5), 670 – 688, 2020. <https://doi.org/10.1080/19648189.2017.1415982>.
- [3] Chen, W., Xu, T., Zhou, W. Microanalysis of smooth Geomembrane–Sand interface using FDM–DEM coupling simulation” *Geotext. Geomembr.*, 49, 276 – 288, 2021. <https://doi.org/10.1016/j.geotextmem.2020.10.022>.
- [4] Pivato, A. Landfill Liner Failure: An Open Question for Landfill Risk Analysis. *J. Environ. Protect.*, 2, 287 – 297, 2017. <https://doi.org/10.4236/jep.2011.23032>.
- [5] Koda, E., Grzyb, M., Osiński, P., Vaverková, M.D. Analysis of failure in landfill and Hydraulic Properties of Three Geosynthetics. *J. Geotech. Geoenviron. Eng.*, 131(8), 937 – 950, 2019.
- [6] Pulat, H.F., Yukselen-Aksoy, Y. Compaction behavior of synthetic and natural MSW samples in different compositions. *Waste. Manag. Res.: J. Sustain. Circ. Econo*, 31(12), 1255 – 1261, 2013. <https://doi.org/10.1177/0734242X13507967>.
- [7] Pulat, H.F., Yukselen-Aksoy, Y. Factors affecting the shear strength behavior of municipal solid wastes. *Waste. Manag.*, 69, 215 – 224, 2017. <https://doi.org/10.1016/j.wasman.2017.08.030>.
- [8] Pulat, H.F., Yukselen-Aksoy, Y. Compressibility and shear strength behaviour of fresh and aged municipal solid wastes. *Environ. Geotech.*, 9(1), 55 – 63, 2022. <https://doi.org/10.1680/jenge.18.00019>.
- [9] Feng, S.J., Cheng, D. Shear strength between soil/geomembrane and geotextile/geomembrane interfaces. *Tunneling and Underground Construction*, Shanghai, China, 26 – 28 May, 558 – 569, 2014.
- [10] Oren, A.H., Ozturk, M., Ozdamar Kul, T., Nart, Z. Barrier performance of geosynthetic clay liners to copper (II) chloride solutions. *Environ. Geotech.*, 7(7), 491 – 500, 2020. <https://doi.org/10.1680/jenge.18.00024>.

- [11] Zhou, L., Zhu, Z., Yu, Z., Zhang, C. Shear Testing of the Interfacial Friction Between an HDPE Geomembrane and Solid Waste. *Mater.*, 13, 1 – 16, 2020. <https://doi.org/10.3390/ma13071672>.
- [12] Ghazizadeh, S., Bareither, C. A. Failure mechanism of geosynthetics clay liner and textured geomembrane composite systems. *Geotext. Geomembr.*, 49, 789 – 803, 2021. <https://doi.org/10.1016/j.geotexmem.2020.12.009>.
- [13] Seed, R. B., Mitchell, J. K., Seed, H. B. *Slope Stability Failure Investigation: Kettleman Hills Repository Landfill Unit B-19, Phase IA*. Berkeley, California: University of California, 1988.
- [14] Brachman, R. W. I., Sabir, A. Geomembrane puncture and strains from stones in an underlying clay layer. *Geotext. Geomembr.*, 28(4), 335-343, 2010.
- [15] Noval, A. M., Blanco, M., Castillo, F., Leiro, A., Mateo, B., Zornberg, J. G., Aguiar, E., Torregrosa, J. B., Redon, M. Long-term Performance of the HDPE Geomembrane at the “San Isidro” Reservoir. In *Proc. 10th Int. Conf. Geosynth.*, Berlin, Germany, 2014.
- [16] Lambert, S., Touze-Foltz, N. A test for measuring permeability of geomembranes. In *Proc. 2nd Europ. Geosynth. Conf.*, Berlin, Germany, 2000.
- [17] Das B. M. 2007. *Principles of foundation engineering*. Sixth edition. Canada: Thomson, 1997.
- [18] Effendi, R. Interface friction of smooth geomembranes and Ottawa sand. *Info Teknik*, 12 (1), 61 – 72, 2011.
- [19] Punetha, P., Mohanty, P., Samanta, M. Microstructural investigation on mechanical behavior of soil – geosynthetic interface in direct shear test. *Geotext. Geomembr.*, 45, 197 – 210, 2017. <https://doi.org/10.1016/j.geotexmem.2017.02.001>.
- [20] Chai, J. C., Saito, A. Interface shear strengths between geosynthetics and clayey soils. *Int. J. Geosyn. Groun. Eng.*, 2 (19), 3 – 9, 2016. <https://doi.org/10.1007/s40891-016-0060-8>.
- [21] Stark, T. D., Santoyo, R. F. Soil/Geosynthetic Interface Strengths from Torsional Ring Shear Tests. In *Proc. Geotech. Front.*, Orlando, Florida, 2017.
- [22] Abdelaal, F., Rowe, R. K., Brachman, R. W. I. Brittle rupture of an aged HDPE geomembrane at local gravel indentation under simulated field conditions. *Geosynth. Int.*, 21(1), 2014. <https://doi.org/10.1680/gein.13.00031>.
- [23] Gulec, B. S., Benson, C. H., Edil, T. B. Effect of Acidic Mine Drainage on the Mechanical construction elements. *MATEC Web of Conferences*, 284, 2005. <https://doi.org/10.1051/mateconf>.
- [24] Mitchell, J. K., Seed, R. B., Seed, H. B. Kettleman Hills waste landfill slope failure. I: Liner-System Properties. *J. Geotech. Eng.*, 116 (4): 647 – 668, 1990. [https://doi.org/10.1061/\(ASCE\)0733-9410\(1990\)116:4\(647\)](https://doi.org/10.1061/(ASCE)0733-9410(1990)116:4(647)).
- [25] Grubb, D., Cheng, S., Dising, W. High altitude exposure testing of geotextiles in the Peruvian Andes. *Geosynthet. Int.*, 6(2), 119 – 144, 1999.

- [26] Ozdamar Kul, T., Oren, A.H. Geosentetik Kil Örtü Hidrasyon Yönteminin Alt Zemin Koşullarına Bağlı Olarak Değerlendirilmesi. *Tek. Der.*, 504, 8385 – 8409, 2018. <https://doi.org/10.18400/tekderg.378245>.
- [27] Polat, F., Ozdamar Kul, T., Oren, A.H. Influence of Mass Per Unit Area on the Hydraulic Conductivity of Geosynthetic Clay Liners (GCLs). *Eur. J. Sci. Tech.*, 28, 1269 – 1273, 2021. <https://doi.org/10.31590/ejosat.1013103>.
- [28] Hrapovic, L. Laboratory Study of Intrinsic Degradation of Organic Pollutants in Compacted Clayey Soil. PhD thesis, The University of Western Ontario, 300, 2001.
- [29] Rowe, R. K. Rimal, S. Aging of HDPE Geomembrane in Three Composite Landfill Liner Configurations. *J. Geotech. Geoenviron. Eng.*, 134(7), 906 – 916, 2008.
- [30] Benson, C., Chen, J., Likos, W., Edil, T. Hydraulic Conductivity of Compacted Soil Liners Permeated with Coal Combustion Product Leachates. *J. Geotech. Geoenviron. Eng.*, 144(4), 2018.
- [31] Rowe, R.K., Rimal, S., Sangam, H. Ageing of HDPE geomembrane exposed to air, water and leachate at different temperatures. *Geotext. Geomembr.*, 27(2), 137 – 151, 2009. <https://doi.org/10.1016/j.geotextmem.2008.09.007>.
- [32] Xie, H., Lou, Z., Chen, Y., Jin, A., Zhan, T.L., Tang, X. An analytical solution to organic contaminant diffusion through composite liners considering the effect of degradation. *Geotext. Geomembr.*, 36, 10 – 18, 2013. <https://doi.org/10.1016/j.geotextmem.2012.10.007>.
- [33] Gulec, S. Effect of acid mine drainage on the properties of geosynthetics.” PhD dissertation, Univ. of Wisconsin-Madison., Madison, Wis, 2003.
- [34] Rowe, R. K., Islam, M. Z., Hsuan, Y. G. Effects of Thickness on the Aging of HDPE Geomembranes. *J. Geotech. Geoenviron. Eng.*, 136 (2): 299-309, 2010. [https://doi.org/10.1061/\(ASCE\)GT.1943-5606.0000207](https://doi.org/10.1061/(ASCE)GT.1943-5606.0000207).
- [35] Maisonneuve, C., Person, P., Duqueno, C., Morin A. Accelerated aging tests for geomembranes used in landfills. Sixth International Landfill Symposium, 207 – 216, 1997.
- [36] ASTM (American Society for Testing and Materials). 2011. Standard Test Method for Direct Shear Test of Soils Under Consolidated Drained Conditions. ASTM D 3080/3080M – 11. West Conshohocken, PA: ASTM.
- [37] Dadkhah, R., Ghafoori, M., Ajalloeian, R., Lashkaripou, G. R. The effect of scale direct shear test on the strength parameters of clayey sand in Isfahan City, Iran. *J. App. Sci.*, 10 (18), 2027 – 2033, 2010. <https://doi.org/10.3923/jas.2010.2027.2033>.
- [38] Sobol, E., Sas, W., Szymanski, A. Scale effect in direct shear tests on recycled concrete aggregate. *Stud. Geotech. Mech.*, 37 (2), 45 – 49, 2015. <https://doi.org/10.1515/sgem-2015-0019>.
- [39] Mohapatra, S. R., Mishra, S. R., Nithin, S., Rajagobal, K. Effect of Box Size on Dilative Behaviour of Sand in Direct Shear Test. In *Proc. Ind. Geotech. Conf.*, 16, 111 – 118: Chennai, India, 2016. [https://doi.org/10.1007/978-981-13-0899-4\\_14](https://doi.org/10.1007/978-981-13-0899-4_14).

- [40] Zahran, K., El Naggar, H. Effect of Sample Size on TDA Shear Strength Parameters in Direct Shear Tests. *Trans. Res. Rec.*, 2674 (9), 1110 – 1119, 2020. <https://doi.org/10.1177/0361198120934482>.
- [41] ASTM (American Society for Testing and Materials). 2020. Standard Test Method for Determining the Shear Strength of Soil – Geosynthetic and Geosynthetic – Geosynthetic Interfaces by Direct Shear. ASTM D 5321/5321M – 20. West Conshohocken, PA: ASTM.
- [42] Shi, J., Shu, S., Qian, X., Wang, Y. Shear strength of landfill liner interface in the case of varying normal stress. *Geotext. Geomembr.*, 48, 713 – 723, 2020. <https://doi.org/10.1016/j.geotexmem.2020.05.004>.
- [43] Koerner, R. M., Martin, J. P., Koerner, G. R. Shear strength parameters between geomembranes and cohesive soils. *Geotext. Geomembr.*, 4(1), 21 – 30, 1986. [https://doi.org/10.1016/0266-1144\(86\)90034-8](https://doi.org/10.1016/0266-1144(86)90034-8).
- [44] Gokhale, A. M. Underwood, E. E. A General Method for Estimation of Fracture Surface Roughness: Part I. Theoretical Aspects. *Metal. Trans. A*, 21A, 1193 – 1199, 1990.
- [45] Gokhale, A. M. Drury, W. J. A General Method for Estimation of Fracture Surface Roughness: Part II. Practical Considerations. *Metal. Trans. A.*, 21A, 1201 – 1207, 1990.
- [46] Vangla, P., Gali, M. L. Shear behavior of sand – smooth geomembrane interfaces through micro – topographical analysis. *Geotext. Geomembr.*, 44, 592 – 603, 2016. <https://doi.org/10.1016/j.geotexmem.2016.04.001>.
- [47] Marcotte, B. A., Fleming, I. R. Direct measurement of geomembrane strain from aggregate indentations. *Geosynt. Int.*, 0 (0), 1 – 54, 2021. <https://doi.org/10.1680/jgein.21.00027>.
- [48] Liu, F., Ying, M., Yuan, G., Wang, J., Gao, Z., Ni, J. Particle shape effects on cyclic shear behaviour of the soil-geogrid interface. *Geotext. Geomembr.*, 49, 991 – 1003, 2021. <https://doi.org/10.1016/j.geotexmem.2021.01.008>.
- [49] Vaid, Y. P., Rinne, N. Geomembrane coefficients of interface friction. *Geosynt. Int.*, 2(1), 309 – 325, 1995.
- [50] Monteiro, C. B., Araújo, G. L. S., Palmeira, E. M., Cordão Neto, M. P. Soil-geosynthetic interface strength on smooth and texturized geomembranes under different test conditions. In *Proc. Int. Conf. Soil Mech. Geotech. Eng.*, 3053 – 3056, Paris, France, 2013.
- [51] Adeleke D., Kalumba D., Nolutshungu L., Oriokot J., Martinez A. The Influence of Asperities and Surface Roughness on Geomembrane/Geotextile Interface Friction Angle. *Int. J. Geosynth. Ground Eng.*, 7(20), 1 – 12, 2021.
- [52] Zettler, T. E., Frost, J. D., DeJong, J. T. Shear-induced changes in smooth HDPE geomembrane surface topography. *Geosynt. Int.*, 7(3), 243 – 267, 2000. <https://doi.org/10.1680/jgein.7.0174>.

- [53] Ling, H. I., Pamuk, A., Dechasakulson, M., Mohri, Y., Burke, C. Interactions between PVC geomembranes and compacted clays. *J. Geotech. Geoenviron. Eng.*, 127, 950 – 954, 2001. [https://doi.org/10.1061/\(ASCE\)1090-0241\(2001\)127:11\(950\)](https://doi.org/10.1061/(ASCE)1090-0241(2001)127:11(950)).
- [54] Yamsani, S. K., Sreedeeep, S., Rakesh, R. R. Frictional and interface frictional characteristics of multi-layer cover system materials and its impact on overall stability. *Int. J. Geosynth. Gro. Eng.*, 2(23), 2 – 9, 2016. <https://doi.org/10.1007/s40891-016-0063-5>.
- [55] Esterhuizen, J. J. B., Filz, G. M., Duncan, J. M. Constitutive behavior of geosynthetic interfaces.” *J. Geotech. Geoenviron. Eng.*, 127, 834 – 840, 2001. [https://doi.org/10.1061/\(ASCE\)1090-0241\(2001\)127:10\(834\)](https://doi.org/10.1061/(ASCE)1090-0241(2001)127:10(834)).
- [56] Stark, T. D., Niazi, F. S., Keuscher, T. C. Strength envelopes from single and multigeosynthetic interface tests. *Geotech. Geo. Eng.*, 33, 1351 – 1367, 2015. <https://doi.org/10.1007/s10706-015-9906-4>.
- [57] Markou, I. N., Evangelou, E. D. Shear Resistance Characteristics of Soil–Geomembrane Interfaces. *Int. J. Geosynth. Gro. Eng.*, 4(29), 1 – 16, 2018. <https://doi.org/10.1007/s40891-018-0146-6>.
- [58] Hsuan, Y., Koerner, R. Antioxidant depletion lifetime in high density polyethylene geomembranes. *J. Geotech. Geoenviron. Eng.*, 124(6), 532 – 541, 1998. [https://doi.org/10.1061/\(ASCE\)1090-0241\(1998\)124:6\(532\)](https://doi.org/10.1061/(ASCE)1090-0241(1998)124:6(532)).
- [59] Kulshreshtha, A. Chemical degradation. *Handbook of polymer degradation*, Dekker, New York, 55–95, 1992.
- [60] Viebke, J., Elble, E., Ifwarson, M., Gedde, U. W. Degradation of unstabilized medium-density polyethylene pipes in hot-water applications. *Polymer Eng. Sci.*, 34(17), 1354 – 1361, 1994. <https://doi.org/10.1002/PEN.760341708>.
- [61] Benson, C., Chen, J., Edil, T. Engineering properties of geosynthetic clay liners permeated with coal combustion product leachates. Rep. No. 3002003770, Electric Power Research Institute, Palo Alto, CA, 2014.
- [62] Salihoglu, H., Chen, J., Likos, W., Benson, C. Hydraulic conductivity of bentonite-polymer geosynthetic clay liners in coal combustion product leachates. Proc., Geo-Chicago 2016: Sustainable Geoenvironmental Systems, ASCE, Reston, VA, 438–448, 2016.
- [63] Frost, J. D., Kim, D., Lee, S. W. Microscale geomembrane-granular material interactions. *KSCE J. Civ. Eng.*, 16 (1), 79 – 92, 2012. <https://doi.org/10.1007/s12205-012-1476-x>.
- [64] Cen, W. J., Wang, H., Fe, Y. J. Laboratory investigation of shear behavior of high – density polyethylene geomembrane interfaces. *Polymers*, 10, 1 – 14, 2018. <https://doi.org/10.3390/polym10070734>.
- [65] Adamska, K. Z. Water content – density criteria for determining geomembrane – fly ash interface shear strength. In Proc. MATEC Web of Conferences, 262, 1 – 8, 2018. <https://doi.org/10.1051/mateconf/201926204005>.

- [66] Khilnani, K., Stark, T. D., Bahadori, T. M. Comparison of Single and Multi Layer Interface Strengths for Geosynthetic/Geosynthetic and Soil/Geosynthetic Interfaces. *Geotech. Front.*, 276, 2017. <https://doi.org/10.1061/9780784480434.005>.
- [67] Isaev, O. N., Sharafutdinov, R. F. Soil Shear Strength at the Structure Interface. *Soil Mech. Found. Eng.*, 57(2), 139 – 146, 2020.
- [68] Cen, W. J., Wang, H., Yu, L., Rahman, M. S. Response of High-Density Polyethylene Geomembrane–Sand Interfaces under Cyclic Shear Loading: Laboratory Investigation. *Int. J. Geomech.*, 20(2), 1 – 15, 2020.
- [69] Cabalar, A. F. Cyclic Behavior of Various Sands and Structural Materials Interfaces. *Geomech. Geoen.*, 10(1), 1 – 19, 2016.